Dynamical Phenomena
at Interfaces, Surfaces
and Membranes


ISBN 1-56072-089-1

# Monte Carlo Study of Vesicles

*S. Komura*[*†] *and A. Baumgärtner*[*]
[*]Institut für Festkörperforschung, Forschungszentrum Jülich, D-5170 Jülich, Germany
[†]Institute of Physics, College of Arts and Sciences, University of Tokyo, Meguro-ku, Tokyo 153, Japan

**Abstract.** Models of self-avoiding polymerized and fluid vesicles are investigated by Monte Carlo simulations. Polymerized vesicles are *not* crumpled and the mean squared radius of gyration is proportional to the number of monomers on the surface, i.e., $R^2 \sim N^\nu$ with $\nu \approx 1.0$. Fluid vesicles, on the other hand, exhibit crumpled shapes with $\nu \approx 0.8$. Polymerized vesicles under constant pressure difference $\bar{p}$ between inside and outside are also studied. Shape transformation to inflated vesicles ($\bar{p} > 0$) and to deflated vesicles ($\bar{p} < 0$) is analyzed by means of finite size crossover scaling assumptions. The crossover to inflated vesicles is governed by the reduction of the roughness on the surface. The crossover to deflated vesicles is ruled by the change of their sizes, i.e., from $\nu \approx 1.0$ to $\nu \approx 0.66$.

## 1. Introduction

Properties of flexible sheet polymer networks have received great attention in connection with both biophysics of membranes and statistical mechanics of random surfaces [1].

A spherically closed membrane is called "vesicle" and is exemplified by red blood cells. This type of thin-walled vesicles are of current interest as models of cell membranes which exhibit many different shapes [2]. This shape transformation is caused by changing, e.g., the osmotic conditions, the composition of the lipid or the temperature. One of the advantages of simulating vesicles instead of open membranes is to remove uncertainties with respect to the boundary effects of open membranes.

In the present proceeding, we report on Monte Carlo studies of polymerized [3,4] and fluid [5-7] vesicles. Polymerized membranes are realized not only in biological

systems, such as, the spectrin protein skeleton of eurythrocytes, but also in artificial membranes, for example, by polymerizing amphiphilic bilayers. In contrast to linear polymer chains, polymerized membranes may exhibit a low temperature flat phase due to phonon-mediated long-range interactions in spite of their two-dimensional character. On the other hand, most of the membranes known in life sciences are fluid. There the configurational arrangement of the monomers represents a distorted surface on which monomers can be able to diffuse freely among each other. We have also investigated polymerized vesicles subjected to osmotic pressure differences

$$\Delta p = p_{\rm in} - p_{\rm out}, \tag{1}$$

measured between inside and outside [8].

Our simulation has been performed in $(d = 3)$-dimensional space, using vesicles which have $(D \equiv d-1 = 2)$-dimensional surfaces (three-dimensional vesicles) as in the real world. The self-avoidance of the surface is also taken into account.

The outline of this article is as following. First we explain the models of polymerized and fluid vesicles and the simulation techniques. In section 3 and 4, we present the results for flaccid polymerized and fluid vesicles, respectively. In section 5, the scaling analysis for polymerized vesicles under constant pressure difference is described.

## 2. Models and Simulation Techniques

The initial configuration of vesicles in $(d = 3)$-dimensional space consists of a triangular mesh as a simplest approximation for $(D = 2)$-dimensional membrane [5,7]. Starting from an icosahedron as the original network, we add new points on each triangle followed by a subsequent rescaling of all bonds to the desired length. This procedure insures that most of the grid points have 6 neighbors and each bond has approximately the same length. In the present simulation we studied vesicles consisting of $N = 10 \times 3^k + 2$ monomers with $k = 1, 2, 3, 4$.

Each Monte Carlo step for vesicles consists of randomly selecting a monomer and displacing it to a nearby location which is chosen also randomly. The energy assigned to a particular configuration of monomers with positions $\{\vec{r}_i\}$ in $(d = 3)$-dimensional space is

$$E = \sum_{\langle i,j \rangle} v(|\vec{r}_i - \vec{r}_j|). \tag{2}$$

Here the summation is over all neighboring pairs of monomers $\langle i, j \rangle$ interacting by a square-well potential, i.e.,

$$v(r) = \begin{cases} 0 & a < r < l_{\rm max} \\ \infty & \text{otherwise.} \end{cases} \tag{3}$$

The parameter $a$ represents the diameter of a hard sphere introduced on each grid point and $l_{\rm max}$ the maximum length of the tether ("tethered" or "polymerized" membrane [3,4]). The self-avoidance of the network and the finite extensibility of the tethers

are maintained by this tethering potential. Furthermore, if $a/l_{\max} > 1/\sqrt{3}$, self-interpenetration of the surface is safely prohibited [3]. In our simulation, $a = 1$ and $l_{\max} = \sqrt{2}a$ are used. Each attempted move of a monomer is set to be $0.1a$ for which about 70% of trials are accepted.

So far we have explained polymerized vesicles and corresponding models for open polymerized membranes have been intensively investigated [9-13]. The connectivity at each monomer is fixed for polymerized vesicles. For fluid vesicles, however, we relax the restriction on the fixed connectivity; we allow the monomers to exchange their neighbors, but still keeping the rule that the topology and integrity of the structure should be preserved.

For a triangular mesh, this can be accomplished by the following simple "triangulation" procedure [5-7]. Four monomers (labeled by 1, 2, 3, 4) which are ringwise connected by four bonds are randomly selected out of $N$ monomers on the surface. Since by construction the surface must be always be covered by triangles, two of the monomers, say 1 and 3, are connected by an additional bond. A triangulation attempt consists in removing this bond and implementing a new one between monomers 2 and 4, which is accepted if $a < l < l_{\max}$. This triangulation procedure is applied to $N$ randomly selected bonds after each Monte Carlo step of monomer displacement. It should be noted that the total numbers of bonds and triangles are always preserved during this bond-exchanging steps.

The actual sampling of configurations is made at least every $N$ Monte Carlo time steps (one Monte Carlo time step corresponds to $N$ attempted moves). Equilibrium averages are taken over up to $10^4$ configurations for both polymerized and fluid vesicles.

## 3. Polymerized Vesicles

A typical equilibrated sample of a polymerized vesicle is depicted in Fig.1 (a). The mean squared radius of gyration, $\langle R^2 \rangle$, and the mean volume, $\langle V \rangle$, of vesicles are expected to scale with the exponents $\nu_R$ and $\nu_V$ as

$$\langle R^2 \rangle \sim N^{\nu_R}, \qquad \langle V \rangle \sim N^{3\nu_V/2}, \tag{4}$$

for large $N$. In general, the exponent $\nu_R$ is not necessarily equal to $\nu_V$. Note that $N$ is proportional to the surface area.

Our Monte Carlo results for $\langle R^2 \rangle$ and $\langle V \rangle$ are

$$\nu_R = 0.95 \pm 0.05, \qquad 3\nu_V/2 = 1.48 \pm 0.04. \tag{5}$$

These results recover our previous simulation for polymerized vesicles [5,7] and, in particular, $\nu_R$ is in good agreement with other simulations for *open* tethered membranes [6,9-12] where $\nu_R \approx 1.0$. We suspect that the difference between the values of $\nu_R$ and $\nu_V$ could be due to finite size effects and we expect $\nu_R = \nu_V = 1.0$ in the asymptotic limit. The fact that the exponents exhibit their upper limiting value ($\nu \leq 1$) implies that polymerized vesicles without any applied pressure are essentially expanded.

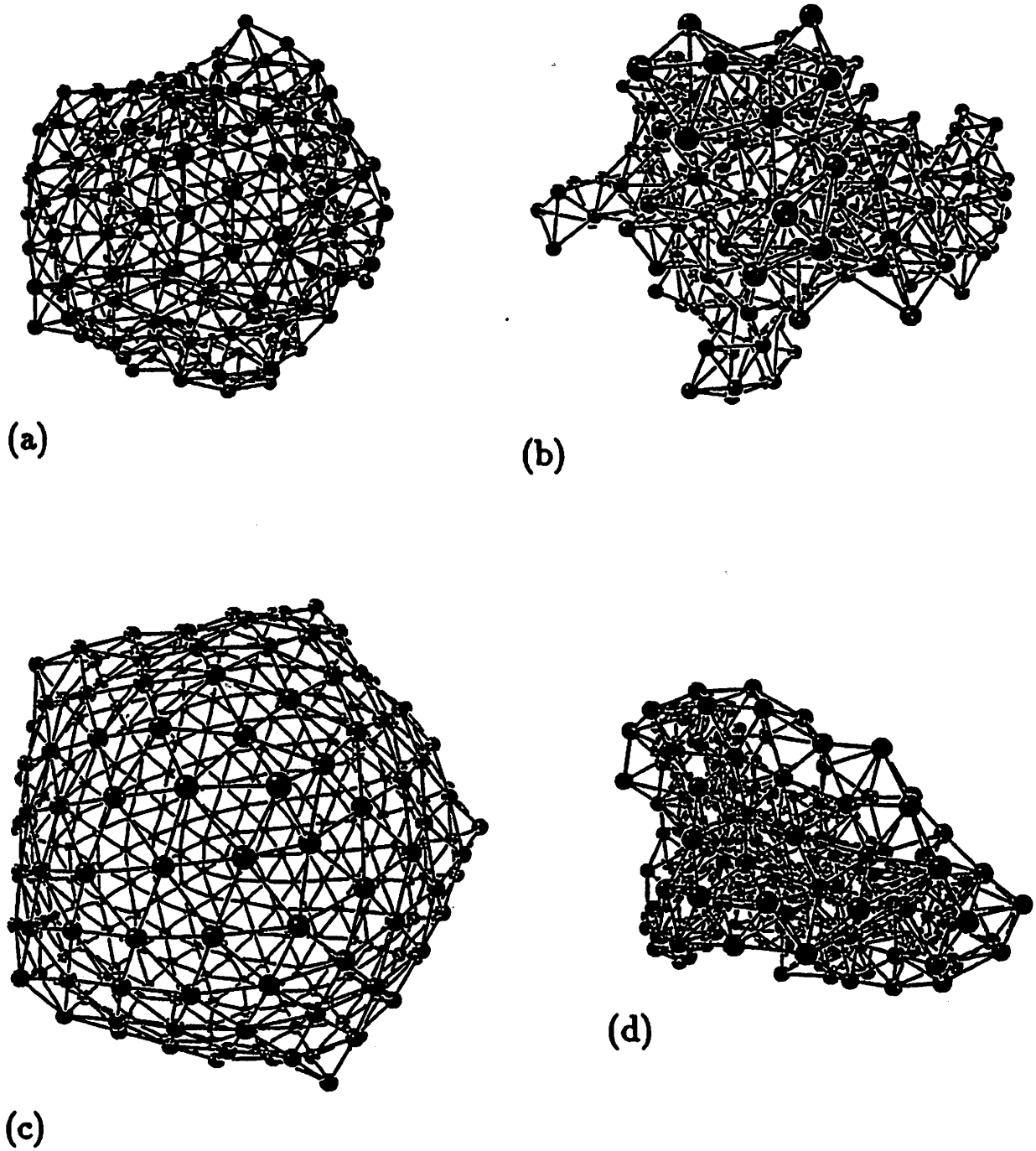


Figure 1. Typical equilibrium configurations of (a) flaccid polymerized vesicle, (b) flaccid fluid vesicle, (c) inflated ($\Delta p a^3/k_B T = 8.0$) polymerized vesicle and (d) deflated ($\bar{p} = -8.0$) polymerized vesicle for $N = 272$. Size of hard spheres is reduced so that the connectivity can be easily seen.

Reasons why self-avoiding tethered surfaces are flat have been suggested very recently by Abraham and Nelson [13]. Due to short range repulsive interactions between adjacent spheres of the membrane, a large bending rigidity is induced in membranes. They showed that this intrinsic bending rigidity is large enough to produce the flat phase.

Although vesicles are in the expanded shapes (with weak asphericity), their conformations are still flaccid and have not reached the fully inflated size. This implies that the surface of flaccid vesicles are substantially rough. The roughness of a surface is generally characterized by the out-of-plane fluctuation $h$ whose squared average scales with the roughness exponent $\zeta$ as [14]

$$\langle h^2 \rangle \sim \frac{k_B T}{\kappa_0} L^{2\zeta}. \tag{6}$$

$L$ is proportional to the linear length scale of the membrane size and $\kappa_0$ is the bending rigidity which, in our case, corresponds to the intrinsic bending rigidity induced by the self-avoidance effect. As mentioned above, tethered surfaces are uncrumpled and one has $L^2 \sim N$. In the case of vesicles, we expect that $\langle h^2 \rangle$ is represented by the fluctuation of the mean square radius of gyration, i.e.,

$$\langle h^2 \rangle \sim \sqrt{\langle (\Delta R^2)^2 \rangle} \equiv \sqrt{\langle R^4 \rangle - \langle R^2 \rangle^2}. \tag{7}$$

The Monte Carlo results for this quantity is $\langle (\Delta R^2)^2 \rangle \sim N^{1.29 \pm 0.16}$. Therefore the roughness exponent is estimated to be $\zeta = 0.645 \pm 0.08$ according to Eqs.(6) and (7). This result is in very good agreement with estimates from previous simulations of open polymerized membranes [6,9,12,13,15,16].

## 4. Fluid Vesicles

A typical equilibrated sample of a fluid vesicle is depicted in Fig.1 (b). The corresponding exponents appearing in Eq.(4) for fluid vesicles are now

$$\nu_R = 0.80 \pm 0.04, \qquad 3\nu_V/2 = 1.23 \pm 0.05. \tag{8}$$

In contrast to polymerized vesicles, Eq.(8) implies that fluid vesicles exhibit properties in agreement with the predicted crumpled phase [17,18]. Ratios of axes of inertia show that fluid vesicles seem to have marked anisotropic ellipsoidal shapes.

The triangulation scheme described in section 2 provides for a given monomer to escape after several bond exchanges from its original neighborhoods of monomers, and hence represents a "fluid" particles. This view is supported by the time dependent mean square displacement of a labeled monomer relative to the motion of the center of mass,

$$r^2(t) = \langle [\vec{r}_k(0) - \vec{r}_{\mathrm{c.m.}}(0) - \vec{r}_k(t) + \vec{r}_{\mathrm{c.m.}}(t)]^2 \rangle, \tag{9}$$

where $\vec{r}_k(t)$ and $\vec{r}_{\mathrm{c.m.}}(t)$ are the position vectors of $k$th monomer and the center of mass at time $t$, respectively. The behavior of $r^2(t)$ is close to $\sim t^{0.8}$ for fluid vesicles while $r^2(t) \sim t^{0.5}$ for polymerized vesicles [5].

## 5. Polymerized Vesicles under Constant Pressure Difference

The energy for polymerized vesicles under constant pressure difference is given by

$$E = -\Delta p \cdot V + \sum_{\langle i,j \rangle} v(|\vec{r}_i - \vec{r}_j|), \tag{10}$$

where $\Delta p$ and $v(r)$ is given by Eqs.(1) and (3), respectively [8]. We fix the pressure difference $\Delta p$ and let the volume $V$ fluctuate in accordance with the Boltzmann weighting factor $\exp(-E/k_BT)$. In other words, we have used the "stress ensemble" [19].

### 5.1. Inflated Regime

When positive or negative constant pressure difference is applied, the shapes of vesicles deviate from flaccid configurations. The related crossover scaling forms are expected to be the analog to those for planar vesicles proposed by Leibler, Singh and Fisher [20,21] and their coworkers [22,23], i.e.,

$$\langle R^2 \rangle \approx N^{\nu} X(x), \qquad \langle V \rangle \approx N^{3\nu/2} Y(x), \tag{11}$$

where $\nu \approx 1.0$ and $x$ is the scaled pressure variable

$$x = \bar{p} N^{\varphi\nu/2}, \qquad \text{with} \quad \bar{p} \equiv \frac{\Delta p a^3}{k_B T}. \tag{12}$$

The crossover exponent $\varphi$ is determined by the fluctuation of the volume at $\bar{p} = 0$ [20,21] and is provided according to the linear response theorem,

$$\langle (\Delta V)^2 \rangle_0 \propto \left( \frac{\partial \langle V \rangle}{\partial \bar{p}} \right)_{\bar{p}=0} \sim N^{(3+\varphi)\nu/2}. \tag{13}$$

By putting $\nu = 1.0$ and using the Monte Carlo result for the fluctuation of the volume which behaves like $\langle (\Delta V)^2 \rangle \sim N^{2.44 \pm 0.13}$, one has $\varphi = 1.88 \pm 0.26$.

For large $\bar{p} > 0$, one expects that the inflated vesicle approaches its sphere-like limiting shape (see Fig.1 (c)). In Fig.2, $X = \langle R^2 \rangle / N^{\nu_R}$ and $Y = \langle V \rangle / N^{3\nu_V/2}$ are plotted according to the crossover scaling form Eq.(11) as a function of $x = \bar{p} N^{\varphi\nu/2}$. Using the estimated crossover exponent $\varphi = 1.88$, one observes the collapsing of all the data to a single curve. This result supports the scaling forms Eq.(11).

It is intuitively clear that the roughness due to the fluctuations of the surface is decreased by increasing the internal pressure. In fact, according to our data $\langle (\Delta R^2)^2 \rangle$ becomes independent of $N$ with increasing $\bar{p}$. Instead of presenting these raw data, we analyzed the fluctuation of the mean squared radius of gyration for various $\bar{p} > 0$ by the crossover scaling form

$$\langle (\Delta R^2)^2 \rangle = N^{2\zeta} f\left(\bar{p} N^{\phi+\zeta}\right). \tag{14}$$

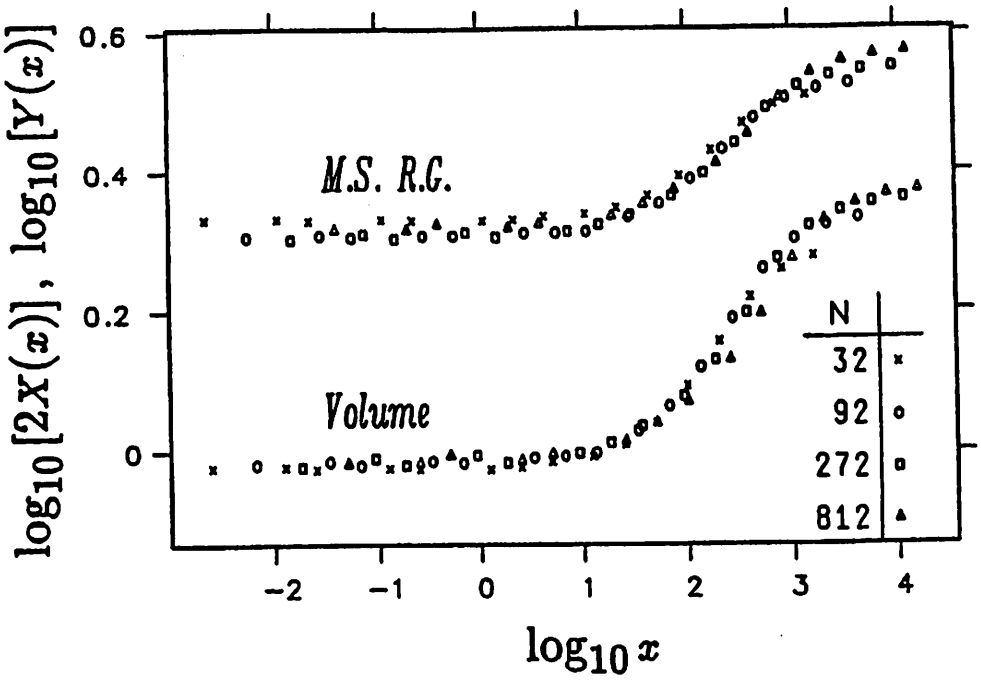


Figure 2. Scaling plots of the mean square radius of gyration and the volume for the inflated ($\bar{p} > 0$) polymerized vesicles. Here $x = \bar{p}N^{\varphi\nu/2}$, $X = \langle R^2\rangle/N^{\nu_R}$ and $Y = \langle V\rangle/N^{3\nu_V/2}$ with $\varphi = 1.88$, $\nu_R = 0.95$ and $\nu_V = 0.99$ are used. $X(x)$ is shifted to avoid the overlap of two curves.

Here $f(y)$ is a scaling function with $f(y) = const.$ for $y \ll 1$. In this limit $\langle(\Delta R^2)^2\rangle$ reduces to flaccid vesicles. Fixing $\zeta = 0.645$, we obtained the best overlap of data if $\phi = 0.05 \pm 0.03$. This is presented in Fig.3, where $f = \langle(\Delta R^2)^2\rangle/N^{2\zeta}$ is shown as a function of $y = \bar{p}N^{\phi+\zeta}$. Our results yield a power law behavior of the scaling function according to $f(y) \sim 1/y^2$ for $y \gg 1$.

### 5.2. Deflated Regime

Monte Carlo results for deflated vesicles with $\bar{p} < 0$ are analyzed by the same crossover scaling forms as given in Eq.(11). However it was necessary to employ a different crossover exponent $\varphi' = 4.40 \pm 0.20$ in order to obtain a collapse of all the data on a single curve. We estimated this value from several attempts to obtain optimal overlap of the curves for all values of $N$. Scaling plots with $\varphi' = 4.40$ is depicted in Fig.4. One observes power laws for $|x| > 10^4$

$$X(x) \approx \frac{X_-}{|x|^\rho}, \qquad Y(x) \approx \frac{Y_-}{|x|^\tau}, \tag{15}$$

with $\rho = 0.140 \pm 0.007$ and $\tau = 0.185 \pm 0.008$. These results imply that $\langle R^2\rangle \sim N^{\nu_R^-}$ and $\langle V\rangle \sim N^{3\nu_V^-/2}$ with $\nu_R^- = \nu_R(1 - \varphi'\rho/2) = 0.66 \pm 0.08$ and $3\nu_V^-/2 = (3\nu_V/2)(1 - \varphi'\tau/3) = 1.08 \pm 0.08$.

Our result for $\nu_R^-$ is very close to the lower limiting value for the exponent $\nu$, corresponding to the "fully collapsed" configuration (see Fig.1 (d)). It is known that

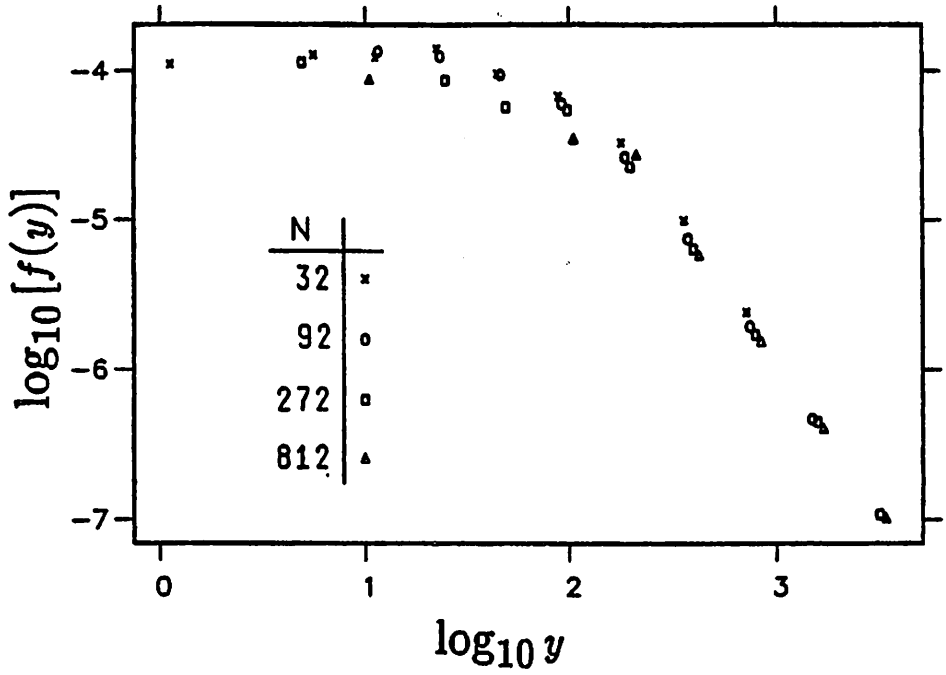


Figure 3. Scaling plot of the fluctuation of mean square radius of gyration for the inflated ($\bar{p} > 0$) polymerized vesicles. Here $y = \bar{p}N^{\phi+\zeta}$ and $f = \langle(\Delta R^2)^2\rangle/N^{2\zeta}$ with $\phi = 0.05$ and $\zeta = 0.645$ are used.

the exponent $\nu$ for a self-avoiding $D$-dimensional surface in $d$-dimensional space should generally satisfy $D/d \leq \nu \leq 1$ which is in our case $2/3 \leq \nu \leq 1$. This compact structure is also observed by the exponent for the volume, $3\nu_V^-/2$, since $\langle V\rangle \sim Na^3$ is expected for this configuration.

It should be noted that the difference between $\varphi' \approx 4.4$ and $\varphi \approx 1.88$ determining crossovers in the deflated and inflated regimes, respectively, is due to the difference in the concerning crossover phenomena; while $\varphi'$ is related to the change of $\nu = 1.0$ to $\nu^- \approx 0.66$, the exponent $\varphi$ is related to the change of $\zeta \approx 0.65$ to $\zeta = 0$.

## Acknowledgements

One of us (S.K.) is very grateful for the hospitality of IFF at Forschungszentrum Jülich. We would like to express our appreciations to Prof. R. Lipowsky and Dr. Y. Taguchi for their interests and useful comments. This work was done on CRAY X-MP/416.

## References

[1] eds, D. R. Nelson, T. Piran and S. Weinberg, *Statistical Mechanics of Membranes and Surfaces (Proc. of the 5th Jerusalem Winter School)* World Scientific, Singapore 1989.

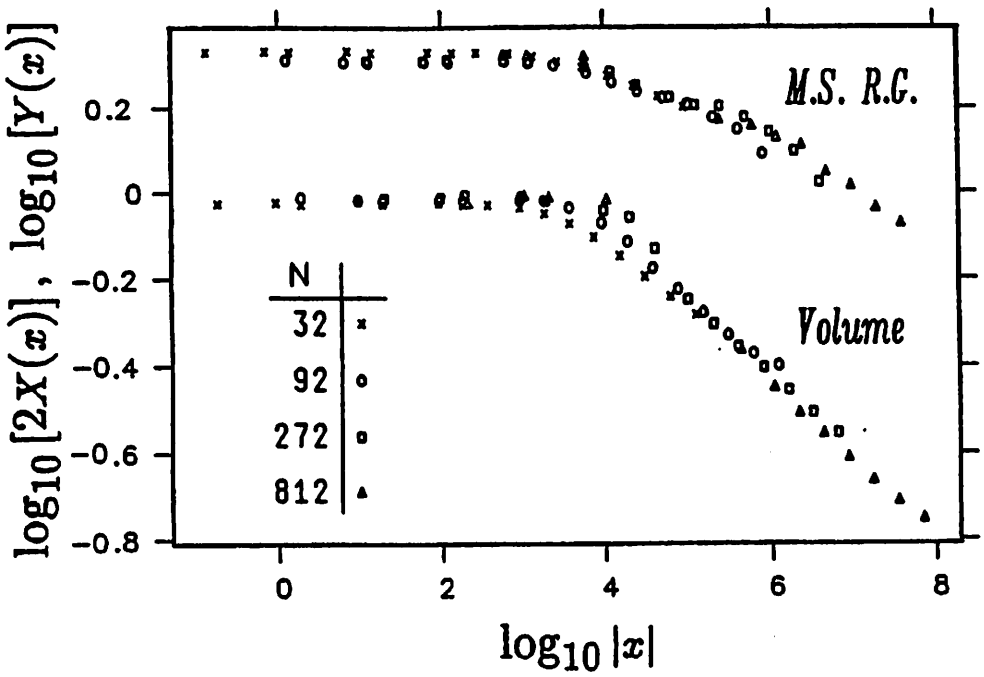


Figure 4. Scaling plots of the mean square radius of gyration and the volume for the deflated ($\tilde{p} < 0$) polymerized vesicles. Here $|x| = |\tilde{p}N^{\varphi'\nu/2}|$, $X = \langle R^2 \rangle / N^{\nu_R}$ and $Y = \langle V \rangle / N^{3\nu\nu/2}$ with $\varphi' = 4.40$, $\nu_R = 0.95$ and $\nu_V = 0.99$ are used. $X(x)$ is shifted to avoid the overlap of two curves.


[2] K. Berndl, J. Käs, R. Lipowsky, E. Sackmann and U. Seifert, *Europhys. Lett.* 13 659 1990.

[3] Y. Kantor, M. Kardar and D. R. Nelson, *Phys. Rev. Lett.* 57 791 1986; *Phys. Rev. A.* 35 3056 1987.

[4] Y. Kantor and D. R. Nelson, *Phys. Rev. Lett.* 58 2774 1987; *Phys. Rev. A.* 36 4020 1987.

[5] A. Baumgärtner and J. -S. Ho, *Phys. Rev. A.* 41 5747 1990.

[6] J. -S. Ho and A. Baumgärtner, *Europhys. Lett.* 12 295 1990.

[7] S. Komura and A. Baumgärtner, *J. Phys. (Paris)* 51 2395 1990.

[8] S. Komura and A. Baumgärtner, *preprint.*

[9] M. Plischke and D. Boal, *Phys. Rev. A.* 38 4943 1988.

[10] F. F. Abraham, W. E. Rudge and M. Plischke, *Phys. Rev. Lett.* 62 1757 1989.

[11] J. -S. Ho and A. Baumgärtner, *Phys. Rev. Lett.* 63 1324 1989.

[12] D. Boal, E. Levinson, D. Liu and M. Plischke, *Phys. Rev. A.* 40 3292 1989.

[13] F. F. Abraham and D R. Nelson, *J. Phys. (Paris)* 51 2653 1990.

[14] R. Lipowsky, *Europhys. Lett.* 7 255 1988.

[15] S. Leibler and A. C. Maggs, *Phys. Rev. Lett.* 63 406 1989.

[16] E. Guitter, S. Leibler, A. C. Maggs and F. David, *J. Phys. (Paris)* 51 1055 1990.

[17] W. Helfrich, *J. Phys. (Paris)* 46 1263 1985.

[18] L. Peliti and S. Leibler, *Phys. Rev. Lett.* 54 1690 1985.

[19] R. M. Neumann, *Phys. Rev. A* 38 4943 1988.

[20] S. Leibler, R. R. P. Singh and M. E. Fisher, *Phys. Rev. Lett.* **59** 1989 1987.
[21] M. E. Fisher, *Physica (Amsterdam)* **38D** 112 1989.
[22] C. J. Camacho and M. E. Fisher, *Phys. Rev. Lett.* **65** 9 1990.
[23] A. C. Maggs, S. Leibler, M. E. Fisher and C. J. Camacho, *Phys. Rev. A.* **42** 691 1990.